An investigation of the Gd-Fe-Cr phase diagram: Phase equilibria at 800 °C

M. Saidi, S. Walha, K. Nouri, A. Kabadou, Lotfi Bessais, M. Jemmali

Version of Record: https://www.sciencedirect.com/science/article/pii/S0925838819312617
Manuscript_0bdaa59dc6913123d9770f931c38a618

An investigation of the Gd-Fe-Cr phase diagram: Phase equilibria at 800°C

M. Saidi,[1,2] S. Walha,[2] K. Nouri,[1,2] A. Kabadou,[2] L. Bessais *,[1] and M. Jemmali[2,3]

[1] *Université Paris Est, ICMPE (UMR 7182), CNRS, UPEC, F-94320 THIAIS France*

[2] *Laboratoire des Sciences des Matériaux et de l'Environnement, Faculté des Sciences de Sfax - Université de Sfax, Sfax, BP 1171, 3018 Tunisie.*

[3] *Chemistry Departement, College of Science and Arts at Ar-Rass, Qassim University, P.O. Box 53, Saudi Arabia.*

Abstract

The phase equilibria of Gd-Fe-Cr system were investigated at 800°C by X-ray powder diffraction (XRD) and scanning electron microscopy (SEM) with energy dispersive spectroscopy (EDS). The isothermal section of the phase diagram consisted of eight single-phase regions, eight two-phase regions and seven three-phase regions. The binary compounds $GdFe_2$, $GdFe_3$, Gd_2Fe_{17}, σ(FeCr) and the ternary compound $GdFe_{10}Cr_2$ were confirmed. Conversely, the binary compound Gd_6Fe_{23} was unstable at the level of 800°C. The maximum solid solubilities of Cr in $GdFe_2$ and Gd_2Fe_{17} were about 11.7 and 13.2 at. % Cr respectively. The compound $GdFe_{12-x}Cr_x$ with the $ThMn_{12}$-type structure (space group $I4/mmm$) has a broad solubility ranging from 15.4 to 23.1 at. % Cr.

PACS numbers:

* Author to whom correspondence should be addressed; electronic mail: bessais @icmpe.cnrs.fr

I. INTRODUCTION

In the last decades, the magnetic refrigeration (MR) based on the magnetocaloric effect (MCE), became the best alternative of the conventional gas-compression refrigeration due to its high thermodynamic efficiency and environmental safety [1–4].

The properties of ternary rare earth iron-rich compounds of the type $RFe_{12-x}M_x$ (R: rare earth metal, M: transition-metal or p-block metal) for (R = Nd, Sm, Gd, Tb, Dy, Ho, Er, Tm, Y and Lu; M= Si, Ti, V, Cr, Mn, Zr, Nb, Mo and W) have been studied intensively [5–13]. This research has been stimulated by the possibility of using some of these materials for high performance applications such as magnetic refrigeration.

Additionally, investigation on the phase diagrams of R-Fe-M systems is still a great concern for researchers in the interest of providing a basis for searching new magnetic materials and improving their performance.

In the R-Fe-M ternary systems the phase equilibrium has already been established for (R = Nd, Sm, Gd, Er and Y; M = Al, Co, Ni, Ge and Ga) [14–18], and in the R-Fe-Cr ternary systems the phase relationships have already been determined for (R = Tb, Dy, Ho, Er and Y) [19–23]. So far, no investigation of the Gd-Fe-Cr ternary system have ever been made.

Thus, the purpose of the present paper is to provide basic information on compound formation and crystal structures of the binary and ternary compounds in the complete isothermal section of the ternary system Gd-Fe-Cr at 800°C.

A detail description of the binary Gd-Fe, Gd-Cr and Fe-Cr phase diagrams was given in references [27–29], with the available crystallographic data and stability temperature range of all the intermediate phases. The Gd-Fe system was investigated in the early 60s by Novy *et al.* [24] who showed the existence of seven binary compounds which have a peritectoid decomposition: Gd_2Fe_{17}, $GdFe_5$, $GdFe_4$, Gd_6Fe_{23}, $GdFe_3$, $GdFe_2$ and Gd_2Fe_3. This binary system was later revised by Copeland *et al.* [25] and Savitskii *et al.* [26]. In 1998, the study of Zhang *et al.* [27] showed that this system comprised four equilibrium intermetallic compounds, namely Gd_2Fe_{17} (Th_2Zn_{17}-type structure), Gd_6Fe_{23} (Th_6Mn_{23}-type structure), $GdFe_3$ ($PuNi_3$-type structure) and $GdFe_2$ ($MgCu_2$-type structure). The Gd-Cr binary phase diagram has been studied by Elliott [28] in 1965 which was based on Copeland and Kato [25]. No binary compounds was found in this phase diagram at 800°C. As for the Fe-Cr binary system, Massalski *et al.* [29] reported that it has only one intermetallic compound

namely σ(FeCr).

The phase diagrams for the three binary systems Gd-Fe [27], Gd-Cr [28],and Fe-Cr [29] adopted in this study are shown in Figure 1.

The ternary compound $GdFe_{10}Cr_2$ was previously identified by Bara *et al.* [11]. This later crystallizes with $ThMn_{12}$-type of the $I4/mmm$ space group.

In this experimental study, the complete isothermal section of the Gd-Fe-Cr ternary system at 800°C was determined.

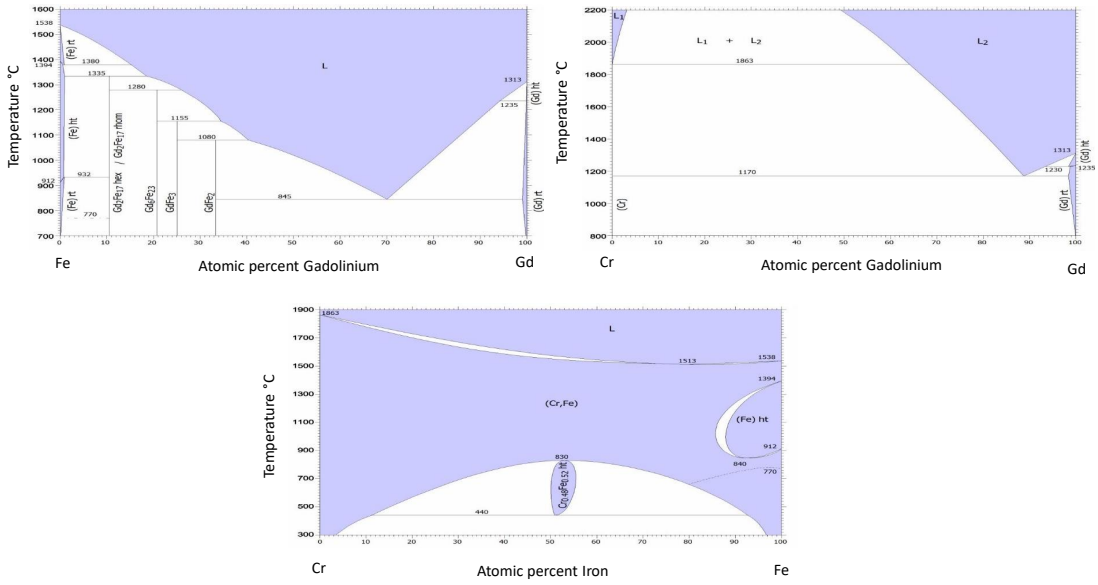

FIG. 1: Gd-Fe, Gd-Cr and Fe-Cr binary phase diagrams.

II. EXPERIMENTAL DETAILS

Bulk metals of gadolinium, iron and chromium, all with purities of 99.99 wt% were respectively used as the starting materials in this work. A total of 75 alloy buttons with weight of 0.5 g each were made in an electric arc furnace under high purity argon using a non-consumable tungsten electrode and a water-cooled cooper crucible. A pure zirconium button was used as an oxygen-getter during the melting process. The alloys were re-melted three to four times, and each time the buttons were turned around in order to attempt complete fusion and ensure homogeneous composition. After alloying, the total mass of each sample was checked. The weight loss was less than 1% of the initial mass. After melting, each ingot

was taken from the furnace, wrapped into tantalum foil, sealed in an evacuated quartz tube and annealed in a tubular furnace at 800°C for 7 days. After the required annealing time, the well-homogenized samples were quenched into ice-water mixture to preserve the high temperature state.

All samples were broken into two parts, one part for X-ray powder diffraction, the other for metallographic investigation. The first part of the samples, was crushed to powders and sieved for XRD analysis while the second part was ground, polished and cleansed in an ultrasonic bath before examination. The X-ray diffraction (XRD) data were collected on a Bruker D8 diffractometer (Bruker AXS, Karlsruhe, Germany) using CuKα radiation ($\lambda_{K\alpha 1}$= 1.540562 Å). Data for Rietveld refinement were collected in the 2θ range from 20° to 80° with a step size of 0.015° and a counting time of 13.5 s per step. The experimental diffraction patterns were compared to those calculated from known structure types using the PowderCell [30] and FullProf [31] softwares.

The metallographic examination was carried out to check the results of X-ray diffraction analysis. Phase identification and composition analysis were investigated by Scanning Electron Microscopy (SEM) with a Silicon Drift Detector (SDD)-X-Max 50 equipped with energy dispersive X-ray spectroscopy (EDS).

III. RESULTS AND DISCUSSION

All the nominal compositions synthesized for the isothermal section Gd-Fe-Cr at 800°C are plotted in Figure 2.

A. Binary systems

Taking into consideration the literature of the previous work [27], four binary compounds, namely Gd_2Fe_{17}, $GdFe_3$, $GdFe_2$ and Gd_6Fe_{23}, were found in the binary system Gd-Fe. In the same binary system studied at 800°C, only the three binary compounds Gd_2Fe_{17}, $GdFe_3$ and $GdFe_2$ were confirmed, but the compound Gd_6Fe_{23} prepared under the same circumstances was unstable, because there were two-phase mixtures containing Gd_2Fe_{17} and $GdFe_3$. As a result, Gd_6Fe_{23} is not stable at 800°C and should not existed in the isothermal section Gd-Fe-Cr. This result is consistent with the findings of our previous work mentioned in

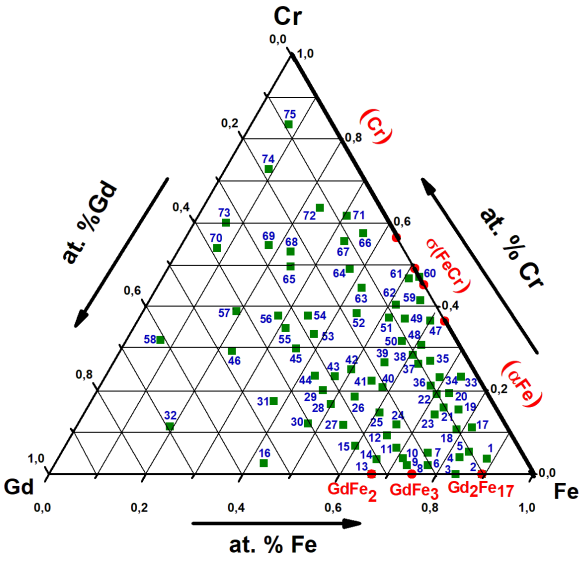

FIG. 2: Prepared compositions of the Gd-Fe-Cr samples.

reference [32].

For the sake of confirming this result, the X-ray diffraction patterns of all the samples prepared in the two-phase regions 5 of the isothermal section Gd-Fe-Cr, showed two-phase equilibrium between Gd_2Fe_{17} and $GdFe_3$. No diffraction reflections which belonged to the phase Gd_6Fe_{23} were observed for these samples, showing no evidence to support the existence of Gd_6Fe_{23} at 800°C. Figure 3 presents the Rietveld refinement of the Gd13-Fe82-Cr5 nominal composition (N° 4 in Figure 2), located in the two-phase region 5 of the ternary phase diagram, consisting of the two phases Gd_2Fe_{17} and $GdFe_3$. The microstructure was examined by SEM and clearly showed the existence of Gd_2Fe_{17} and $GdFe_3$, as presented in Figure 4. The darker grey areas show the phase Gd_2Fe_{17} and the bright grey areas show the phase $GdFe_3$.

The Rietveld analysis of the binary compound $GdFe_2$ is represented in Figure 5. The lattice parameter for this phase was: $a = 7.380(5)$ Å.

The Gd_2Fe_{17} compound displays two polymorphic forms: hexagonal with $P6_3/mmc$ space group (Th_2Ni_{17}-type structure) and rhombohedral with $R\bar{3}m$ space group (Th_2Zn_{17}-type structure) [33]. In this study, the peaks of the X-ray diffraction pattern of this sample were indexed with the rhombohedral unit-cell. Figure 6 shows the Rietveld refinement for the binary Gd_2Fe_{17}. This analysis proves that this intermetallic compound adopts the

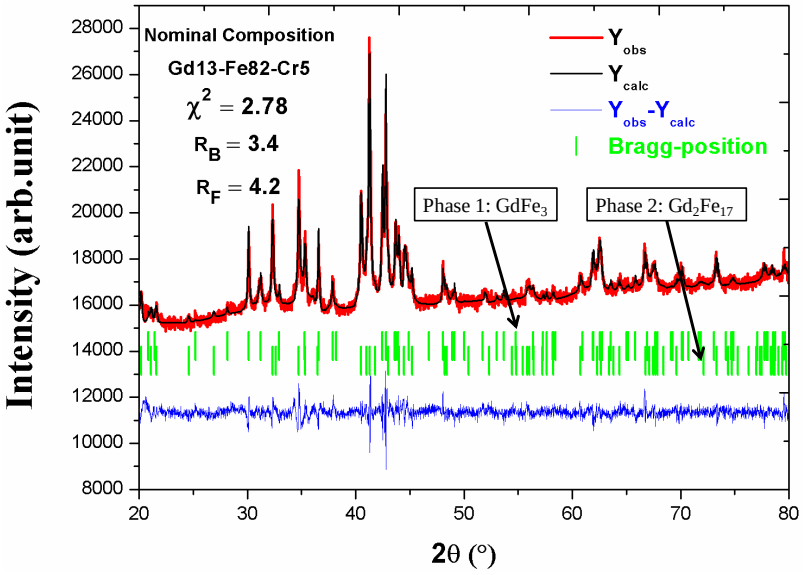

FIG. 3: Rietveld analysis for X-ray diffraction pattern of the Gd13-Fe82-Cr5 nominal composition.

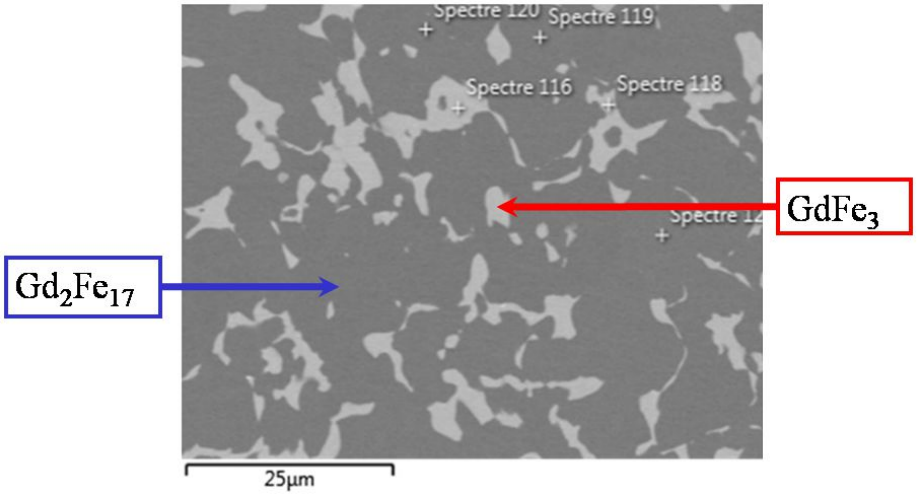

FIG. 4: Backscattered electron SEM image of the Gd13-Fe82-Cr5 nominal composition showing the presence of the phases Gd_2Fe_{17} and $GdFe_3$.

rhombohedral Th_2Zn_{17} structure with $R\bar{3}m$ space group, and the lattice parameters were: $a = 8.513(6)$ Å and $c = 12.453(2)$ Å.

A series of samples near the σ(FeCr)-phase region were prepared in the Fe-Cr binary system, in order to confirm the existence of the σ(FeCr) phase. The results of X-ray diffraction show that these samples had patterns of σ(FeCr). Therefore, it was confirmed that the σ(FeCr) phase exists in the Fe-Cr binary system at 800°C with a narrow homogeneity range

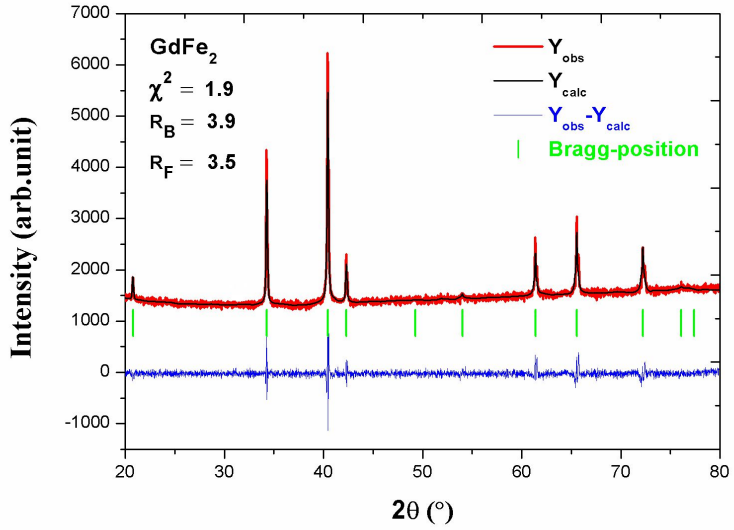

FIG. 5: Rietveld analysis for X-ray diffraction pattern of $GdFe_2$ binary compound.

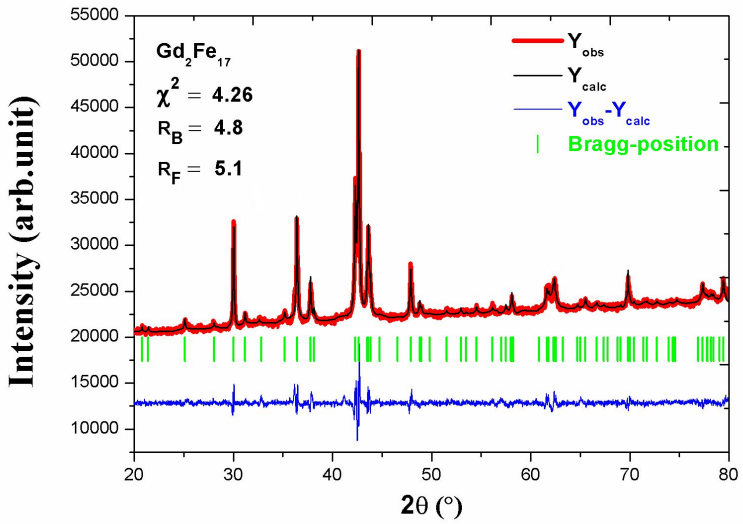

FIG. 6: Rietveld analysis of Gd_2Fe_{17} binary compound.

of 45.3-49 at. % Cr.

B. Ternary system

The phase RFe_{12} is based on the tetragonal $ThMn_{12}$-type structure, with the $I4/mmm$ space group [34]. In this structure, the rare earth Th atoms occupied the 2a (0,0,0) site and the Mn atoms occupy three crystallographic non-equivalent sites, denoted as Mn (8i), Mn (8j) and Mn (8f): 8i (x, 0, 0), 8j (x, 1/2, 0) and 8f (1/4, 1/4, 1/4) [35]. Figure 7 shows the crystal structure of $ThMn_{12}$.

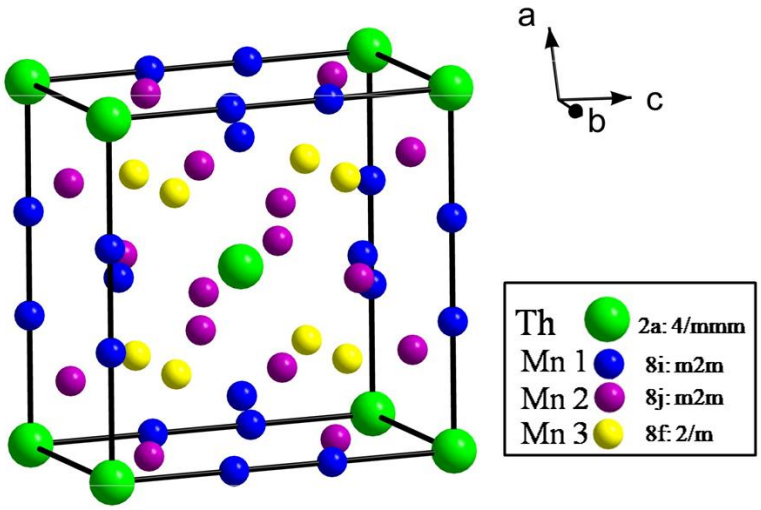

FIG. 7: Tetragonal crystal structure of $ThMn_{12}$ [35].

It is well known [5–13] that the pure phase RFe_{12} is not stable and the addition of a transition metal or a p-block metal M (M = Si, Ti, V, Cr, Mn, Zr, Nb, Mo and W) is necessary to stabilize the $ThMn_{12}$ structure and form the $RFe_{12-x}M_x$ compounds. In the current research, and by analyzing and comparing the X-ray diffraction patterns and micrographs, the existence of the ternary compound $GdFe_{10}Cr_2$ was confirmed. The Rietveld refinement for the XRD pattern of the compound $GdFe_{10}Cr_2$ with cell parameters a = 8.480(6) Å and c = 4.755(3) Å, is shown in Figure 8.

Crystal structure and lattice parameter data of the binary and ternary phases are given in Table I with references.

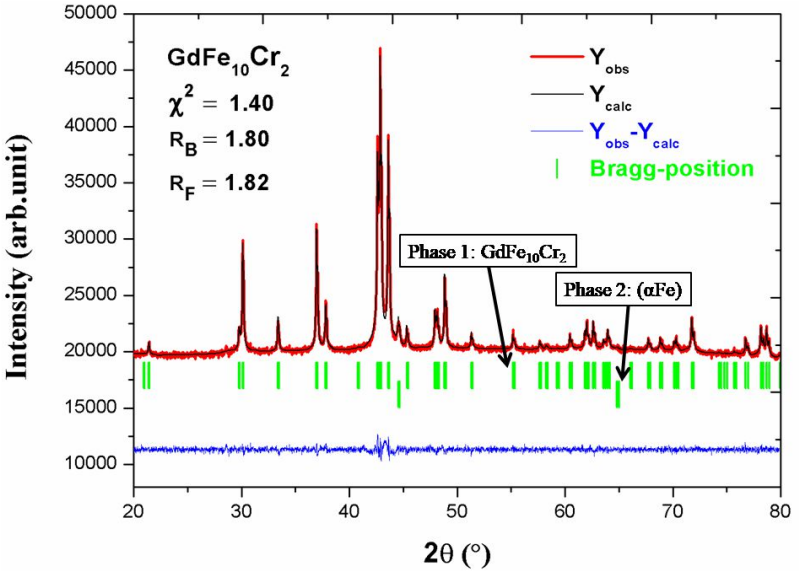

FIG. 8: Rietveld analysis of $GdFe_{10}Cr_2$ annealed at 800°C. The ticks refer to the main phase and (αFe).

TABLE I: Crystallographic data of intermetallic compounds in Gd-Fe-Cr ternary system at 800 °C.

Phase	Structure	Space	Lattice parameters (Å)		References
Composition	type	group	a	c	
$GdFe_{10}Cr_2$	$ThZn_{12}$	$I4/mmm$	8.507	4.769	[11]
$GdFe_{10}Cr_2$	$ThZn_{12}$	$I4/mmm$	8.480(6)	4.755(3)	This work
Gd_2Fe_{17}	Th_2Zn_{17}	$R\bar{3}m$	8.510	12.510	[36]
Gd_2Fe_{17}	Th_2Zn_{17}	$R\bar{3}m$	8.513(6)	12.453(2)	This work
$GdFe_3$	$PuNi_3$	$R\bar{3}m$	5.148	24.62	[37]
$GdFe_3$	$PuNi_3$	$R\bar{3}m$	5.166(4)	24.705(1)	This work
$GdFe_2$	$MgCu_2$	$Fd\bar{3}m$	7.390	-	[38]
$GdFe_2$	$MgCu_2$	$Fd\bar{3}m$	7.380(5)	-	This work
σ(FeCr)	W	$Im\bar{3}m$	2.863	-	[39]
Gd	Mg	$P6_3/mmc$	3.634	5.785	[40]
(αFe)	W	$Im\bar{3}m$	2.868	-	[41]
Cr	Cr	$Im\bar{3}m$	2.899	-	[42]

C. Solid solubility

According to the results obtained from SEM/EDS combined with the X-ray diffraction technique, the extended regions of solid solubility of each single phase in the 800°C isothermal section were clearly identified. The Gd-Fe-Cr phase diagram was characterized by a large homogeneity ranges covering the iron-rich region which is summarized in Table II.

In order to identify the $Gd(Fe,Cr)_2$ solid solution at 800°C, several samples on this binary extension and in the regions either side were synthesized. The existence of the $GdFe_{2-x}Cr_x$ solid solution was proven by the two samples with nominal compositions Gd44-Fe37-Cr19 and Gd18-Fe44-Cr38 prepared respectively in the three phase-region A and the two-phase region 1 of the Gd-Fe-Cr ternary phase diagram. The XRD pattern (Figure 9) of the Gd44-Fe37-Cr19 composition (N° 31 in Figure 1) showed a three-phase equilibrium between the upper limit of the solid solution $GdFe_{2-x}Cr_x$ ($x = 0.35$), (Gd) and (Cr). This result was confirmed by the microstructure in Figure 10.

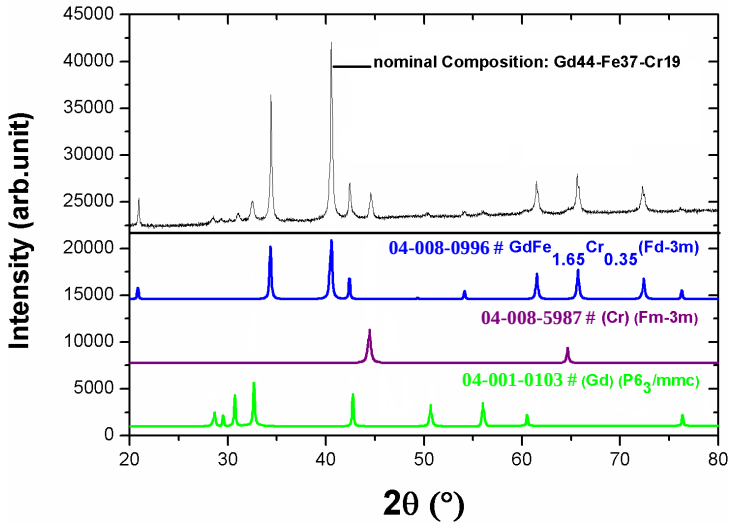

FIG. 9: Experimental XRD pattern of the Gd44-Fe37-Cr19 composition showing the equilibrium between $GdFe_{1.65}Cr_{0.35}$, (Gd) and (Cr) phases.

Similarly, the X-ray powder pattern and the microstructure of the Gd18-Fe44-Cr38 composition (N° 52 in Figure 1), which was melted and heat-treated at 800°C, revealed a solid state equilibrium between the upper limit of the solid solution $GdFe_{2-x}Cr_x$ ($x = 0.35$) and (Cr). The powder pattern of the Gd18-Fe44-Cr38 composition is given in Figure 11. In the SEM image (Figure 12), the light grey area had an atomic composition in agreement with

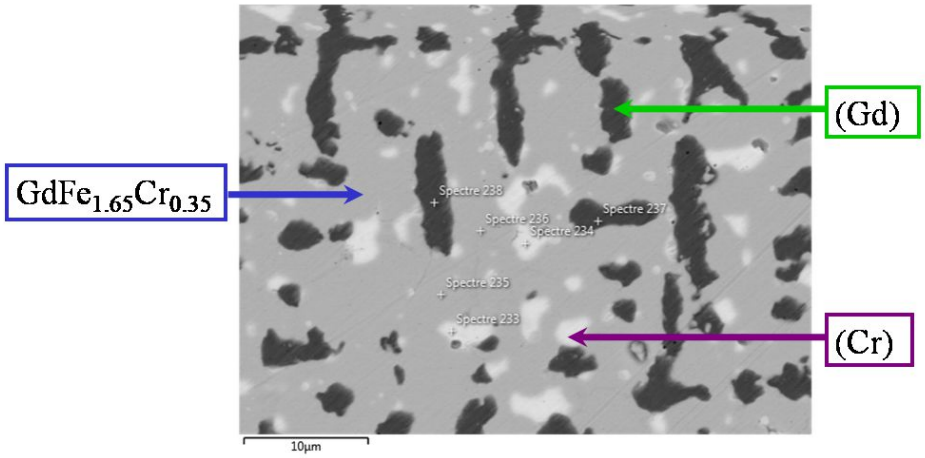

FIG. 10: Backscattered electron SEM image of the Gd44-Fe37-Cr19 sample showing the equilibrium between $GdFe_{1.65}Cr_{0.35}$, (Gd) and (Cr) phases.

$GdFe_{1.65}Cr_{0.35}$, and the dark grey area presented an atomic composition in agreement with (Cr).

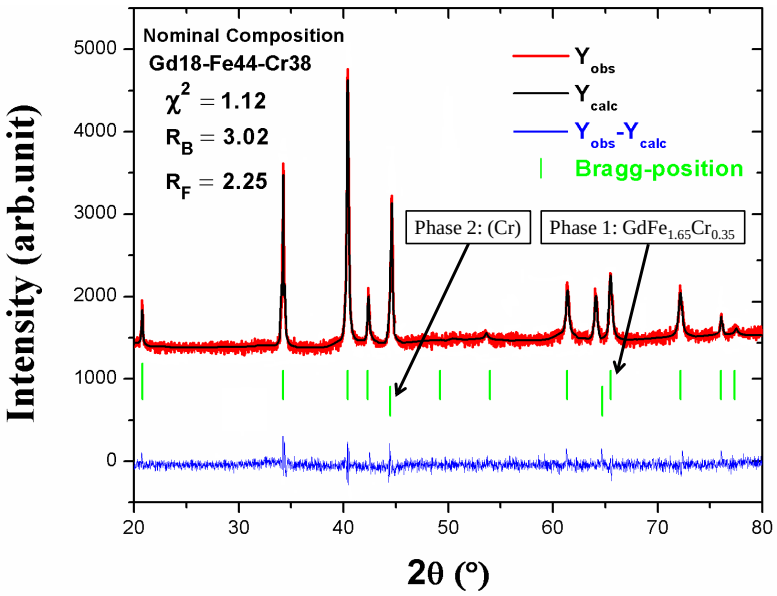

FIG. 11: Rietveld analysis for X-ray diffraction pattern of the Gd18-Fe44-Cr38 composition. All the diffraction peaks were indexed with both the cubic structures of $GdFe_{1.65}Cr_{0.35}$ and (Cr).

Both SEM-EDS and X-ray diffraction showed that the solubility of Cr in the $GdFe_2$ cubic Laves C15 phase ($MgCu_2$-type structure, $Fd\bar{3}m$ space group) extended from the $GdFe_{2-x}Cr_x$ ($x = 0$) compound ($a = 7.380(5)$ Å) to the $GdFe_{2-x}Cr_x$ ($x = 0.35$) compound ($a = 7.398(3)$

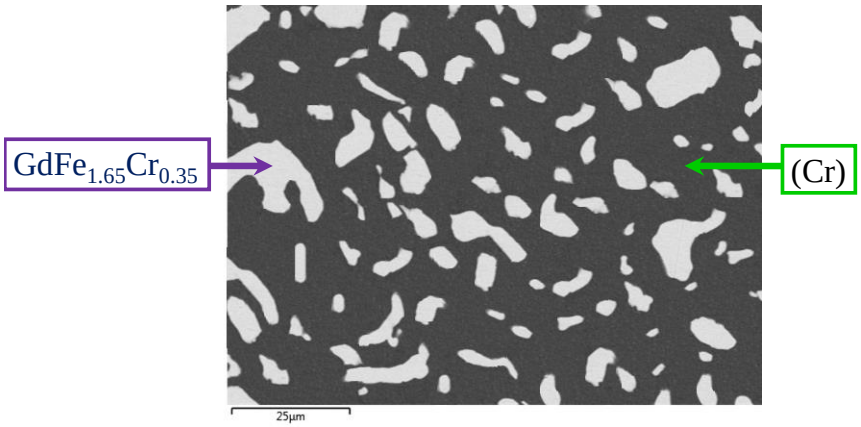

FIG. 12: Backscattered electron SEM image of the microstructure of the sample with nominal composition Gd18-Fe44-Cr38 showing the equilibrium between $GdFe_{1.65}Cr_{0.35}$ and (Cr).

Å) (Table II). Figure 13 presents the Rietveld refinement of the $GdFe_{2-x}Cr_x$ $x = 0.1$ and $x = 0.27$ series. During the study of this homogeneity domain, the same type of structure of $MgCu_2$ was retained.

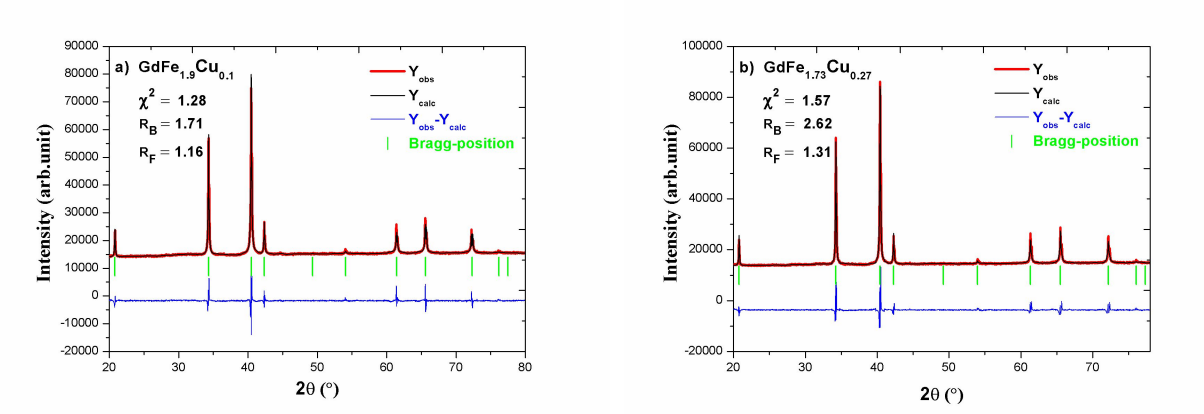

FIG. 13: Rietveld analysis of $GdFe_{2-x}Cr_x$ compounds: a) $x = 0.1$, and b) $x = 0.27$.

The stability of the $Gd_2Fe_{17-x}Cr_x$ solid solution was confirmed using the SEM-EDS and the X-ray difraction. The synthesis of the Gd25-Fe64-Cr11 nominal composition (N° 12 in Figure 2) in the three phase-region G of the Gd-Fe-Cr ternary phase diagram, revealed the limit of this solid solution. The XRD pattern (Figure 14) and the SEM micrograph (Figure 15) of the Gd25-Fe64-Cr11 sample clearly shows a three-phase equilibrium between the upper limit of the solid solution $Gd_2Fe_{17-x}Cr_x$ ($x = 2.5$), the upper limit of the solid solution $GdFe_{2-x}Cr_x$ ($x = 0.35$) and the phase $GdFe_3$. In Figure 16, the dark area was

identified as $Gd_2Fe_{14.5}Cr_{2.5}$, the medium grey area as $GdFe_3$, while the light grey area as $GdFe_{1.65}Cr_{0.35}$.

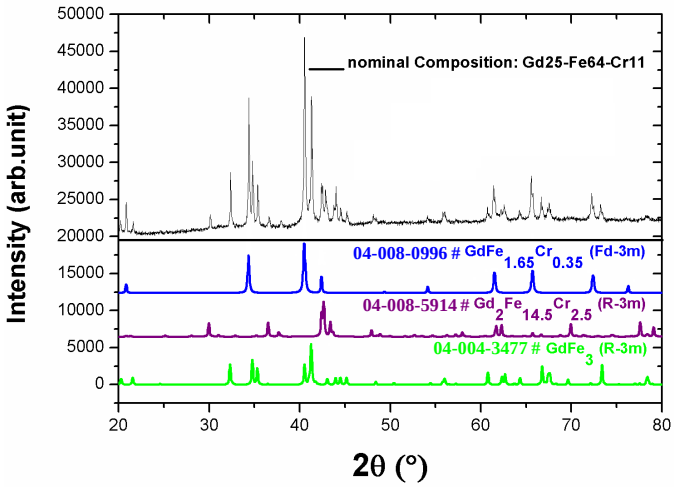

FIG. 14: Experimental XRD pattern of the Gd25-Fe64-Cr11 composition showing the equilibrium between $Gd_2Fe_{17-x}Cr_x (x = 2.5)$, $GdFe_{2-x}Cr_x$ $(x = 0.35)$ and $GdFe_3$.

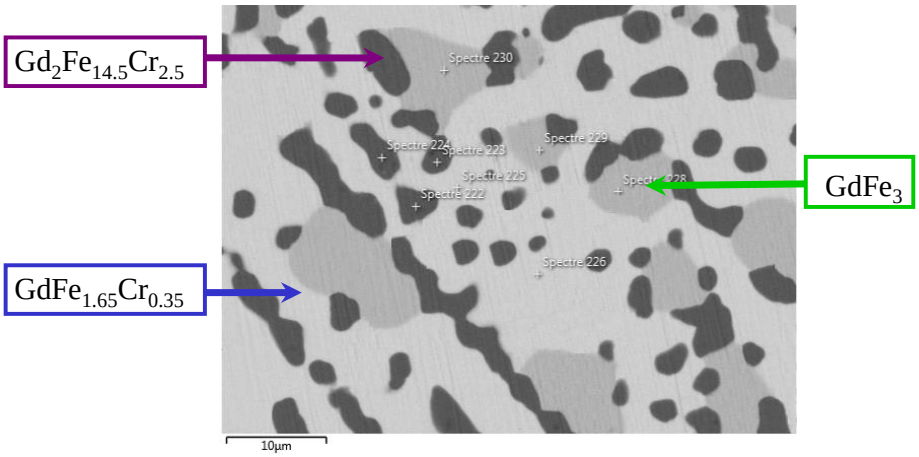

FIG. 15: Backscattered electron SEM image of the Gd25-Fe64-Cr11 sample showing the equilibrium between $Gd_2Fe_{17-x}Cr_x (x = 2.5)$, $GdFe_{2-x}Cr_x$ $(x = 0.35)$ and $GdFe_3$.

The maximum solid solubility of Cr in $Gd_2Fe_{17-x}Cr_x$ was determined to be around 13.2 at. % Cr (Table II). The Rietveld analysis of the $Gd_2Fe_{17-x}Cr_x$ $x = 1$ and $x = 2$ series are represented in Figure 16. The lattice parameters for $Gd_2Fe_{16}Cr_1$ were: $a = 8.544(2)$ Å and $c = 12.443(9)$ Å and the lattice parameters for $Gd_2Fe_{15}Cr_2$ were: $a = 8.549(2)$ Å and $c = 12.452(3)$ Å.

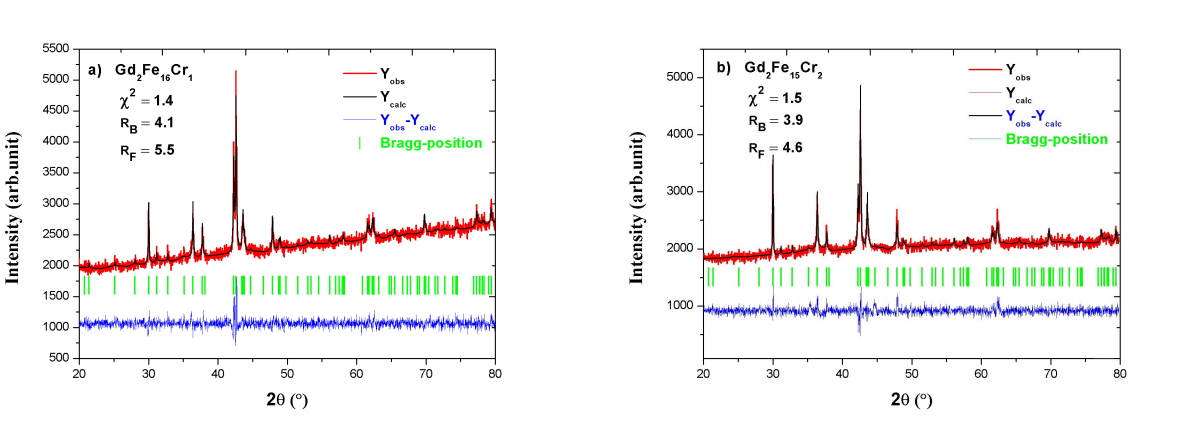

FIG. 16: Rietveld analysis of $Gd_2Fe_{17-x}Cr_x$ compounds: a) $x = 1$, and b) $x = 2$ as an example.

The existence of the ternary line compound $GdFe_{12-x}Cr_x$ was revealed by annealed samples of several compositions. The analysis of the results of the scanning electron microscope coupled to the X-ray diffractograms of each sample allowed the delimitation of the $GdFe_{12-x}Cr_x$ ternary solid solution. The homogeneity range of the $GdFe_{12-x}Cr_x$ solid solution, which crystallizes in the tetragonal $ThMn_{12}$ type-structure with the $I4/mmm$ space group, extended from about 15.4 at. % Cr to 23.1 at. % Cr at 800°C (Table II). The SEM image (Figure 17) for the Gd8-Fe81-Cr11 nominal composition (N° 17 in Figure 2) located in the three-phase region F of the ternary phase diagram, shows the thermodynamic equilibrium between the lower limit of the $GdFe_{12-x}Cr_x$ solid solution which is $GdFe_{10}Cr_2$, the upper limit of the $Gd_2Fe_{17-x}Cr_x$ ($x = 2.5$) solid solution and (αFe).

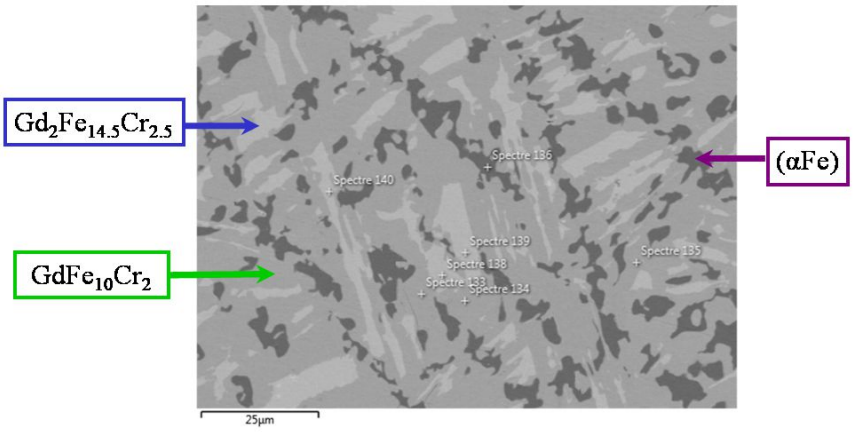

FIG. 17: Backscattered electron SEM image of the Gd8-Fe81-Cr11 sample showing the equilibrium between $GdFe_{10}Cr_2$, $Gd_2Fe_{14.5}Cr_{2.5}$ and (αFe) phases.

The experimental X-ray diffractogram (Figure 18) of the Gd11-Fe61-Cr28 nominal composition (N° 38 in Figure 2) located in the three-phase region C of the Gd-Fe-Cr ternary system, was indexed to three type structures, and shows the three-phase equilibrium between the following phases: $GdFe_{2-x}Cr_x$ ($x = 0.35$) ($MgCu_2$-type structure) + $GdFe_{12-x}Cr_x$ ($x = 3$) ($ThMn_{12}$-type structure) + σ(FeCr) (W-type structure). The SEM image cofirmed this result (Figure 19).

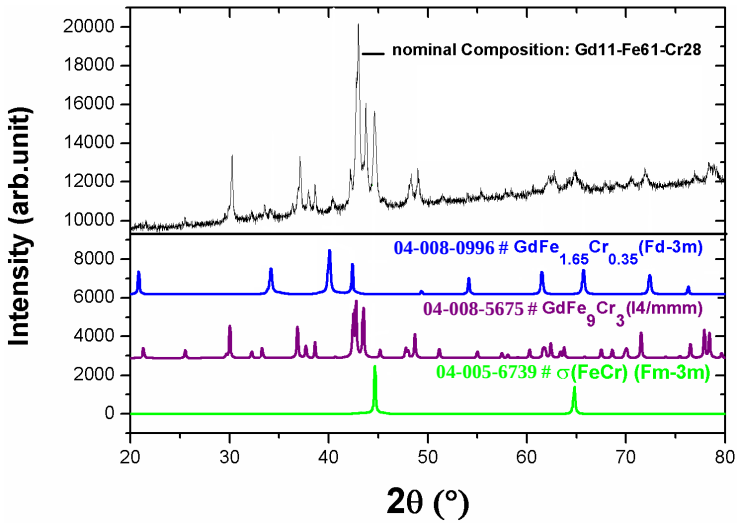

FIG. 18: X-ray diffraction pattern of the Gd11-Fe61-Cr28 composition.

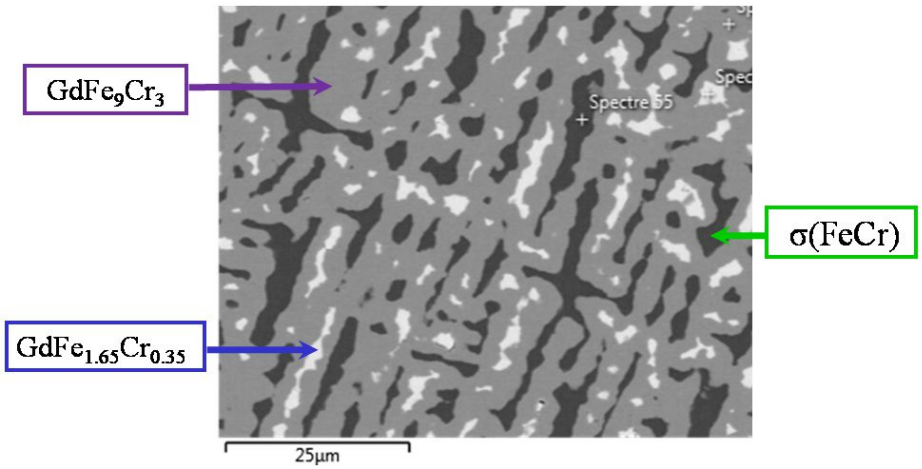

FIG. 19: Backscattered electron SEM image of the Gd11-Fe61-Cr28 composition.

Furthermore, metals Fe and Cr can substitute each other and form a solid solution, as shown in the Fe-Cr binary phase diagram. Cr was found to dissolve up to 35.9 at. % Fe,

TABLE II: Lattice parameters and homogeneity ranges of the identified solid solutions in the Gd-Fe-Cr system at 800°C.

Phase	Homogeneity ranges	Lattice parameters (Å)	
		a	c
$GdFe_{2-x}Cr_x$	$(0 \leq x \leq 0.35)$		
$x = 0$		7.380(5)	-
$x = 0.1$		7.385(8)	-
$x = 0.2$		7.388(3)	-
$x = 0.27$		7.397(5)	-
$x = 0.35$		7.398(3)	-
$Gd_2Fe_{17-x}Cr_x$	$(0 \leq x \leq 2.5)$		
$x = 0$		8.513(6)	12.453(2)
$x = 0.5$		8.543(2)	12.436(8)
$x = 1$		8.544(2)	12.443(9)
$x = 2$		8.549(2)	12.452(3)
$x = 2.5$		8.556(5)	12.466(4)
$GdFe_{12-x}Cr_x$	$(2 \leq x \leq 3)$		
$x = 2$		8.480(6)	4.755(3)
$x = 2.5$		8.485(1)	4.756(7)
$x = 3$		8.487(8)	4.757(3)

while Fe was found to extend up to 43.5 at. % Cr. The σ(FeCr) compound has a narrow homogeneity range of 45.3-49 at. % Cr in the binary Fe-Cr.

D. Phase equilibrium at 800°C

From the combination of XRD analysis and SEM-EDS results obtained from 75 binary and ternary samples, the phase equilibria in the Gd-Fe-Cr ternary system were identified and the 800°C isothermal section was constructed (Figure 20). A total of four binary compounds, namely $GdFe_2$, $GdFe_3$, Gd_2Fe_{17} and σ(FeCr) were characterized.

This study has enabled the determination of three solid solutions, and the characterization

of divers equilibrium areas. All binary phases of the Gd-Fe binary system extended into the ternary, except $GdFe_3$. The $GdFe_{2-x}Cr_x$ and $Gd_2Fe_{17-x}Cr_x$ solid solutions showed maximum extensions up to $x = 0.35$ and $x = 2.5$ respectively. Also, the Gd-Fe-Cr system contained one ternary solid solution $GdFe_{12-x}Cr_x$, having small homogeneity domain which extended from the $GdFe_{12-x}Cr_x$ $(x = 2)$ composition to the $GdFe_{12-x}Cr_x$ $(x = 3)$ composition.

The determined phase relationship indicates that the isothermal section of the Gd-Fe-Cr ternary system at 800°C consists of eight single-phase regions, eight two-phase regions and seven three-phase regions. In order to further identify these phase relationships, Table III and Table IV present respectively the details of the measured compositions by EDS with their numbers as shown in Figure 2 in the two-phase regions and three-phase regions of the Gd-Fe-Cr ternary system.

TABLE III: Phase compositions of the two-phase regions in the Gd-Fe-Cr ternary system at 800°C.

Phase regions	No	Nominal compositions	Phases	EDS results (at.%)		
				Gd	Fe	Cr
1	52	Gd18-Fe44-Cr38	(Cr)	0.0	40	60
			$GdFe_{1.65}Cr_{0.35}$	33.1	55.2	11.7
2	59	Gd2-Fe52-Cr42	σ(FeCr)	0.0	52.2	47.8
			$GdFe_9Cr_3$	7.7	69.2	23.1
3	33	Gd4-Fe73-Cr23	(αFe)	0.0	59.8	40.2
			$GdFe_{10}Cr_2$	7.7	76.9	15.4
4	1	Gd7.2-Fe88.7-Cr3.7	$Gd_2Fe_{14.5}Cr_{2.5}$	10.5	76.3	13.2
			(αFe)	0.0	99.7	0.3
5	7	Gd19-Fe77-Cr4	$Gd_2Fe_{14.5}Cr_{2.5}$	10.5	76.4	13.1
			$GdFe_3$	25	75	0.0
6	25	Gd24-Fe62-Cr14	$GdFe_{1.65}Cr_{0.35}$	33.1	55.3	11.6
			$GdFe_{9.5}Cr_{2.5}$	7.7	73.1	19.2
7	14	Gd30-Fe66-Cr4	$GdFe_{1.65}Cr_{0.35}$	33.2	55.2	11.6
			$GdFe_3$	24.8	75.2	0.0
8	16	Gd54-Fe43-Cr3	$GdFe_{1.65}Cr_{0.35}$	33.1	55.1	11.8
			(Gd)	99.9	0.1	0.0

TABLE IV: Phase compositions of the three-phase regions in the isothermal section of Gd-Fe-Cr ternary system at 800°C.

Phase regions	No	Nominal compositions	Phases	EDS results (at.%)		
				Gd	Fe	Cr
A	31	Gd44-Fe37-Cr19	(Gd)	99.8	0.0	0.2
			$GdFe_{1.65}Cr_{0.35}$	33.2	55.1	11.7
			(Cr)	0.3	0.0	99.7
B	51	Gd10-Fe51-Cr39	σ(FeCr)	0.0	51	49
			$GdFe_{1.65}Cr_{0.35}$	33.2	55.1	11.7
			(Cr)	0.0	39.8	60.2
C	38	Gd11-Fe61-Cr28	$GdFe_9Cr_3$	7.7	69.4	22.9
			$GdFe_{1.65}Cr_{0.35}$	33.3	55.3	11.4
			σ(FeCr)	0.0	51.8	48.2
D	47	Gd2-Fe60-Cr38	(αFe)	0.0	60	40
			σ(FeCr)	0.0	54.7	45.3
			$GdFe_9Cr_3$	7.7	69.3	23
E	21	Gd10-Fe75-Cr15	$GdFe_{10}Cr_2$	7.7	77	15.4
			$Gd_2Fe_{14.5}Cr_{2.5}$	10.5	76.2	13.3
			$GdFe_{1.65}Cr_{0.35}$	33.3	55.2	11.5
F	17	Gd8-Fe81Cr11	$GdFe_{10}Cr_2$	7.6	77	15.4
			$Gd_2Fe_{14.5}Cr_{2.5}$	10.6	76.2	13.2
			(αFe)	0.0	99.8	0.2
G	12	Gd25-Fe64-Cr11	$GdFe_3$	24.9	75.1	0.0
			$Gd_2Fe_{14.5}Cr_{2.5}$	10.5	76.3	13.2
			$GdFe_{1.65}Cr_{0.35}$	33.2	55	11.8

In this work, by comparing and analyzing the XRD experiments and SEM/EDS examinations of all the samples and identifying the phases in each composition, the isothermal section of the Gd-Fe-Cr ternary system at 800°C was constructed (Figure 20). The complete investigation of the Gd-Fe-Cr phase diagram confirms the literature data and provides

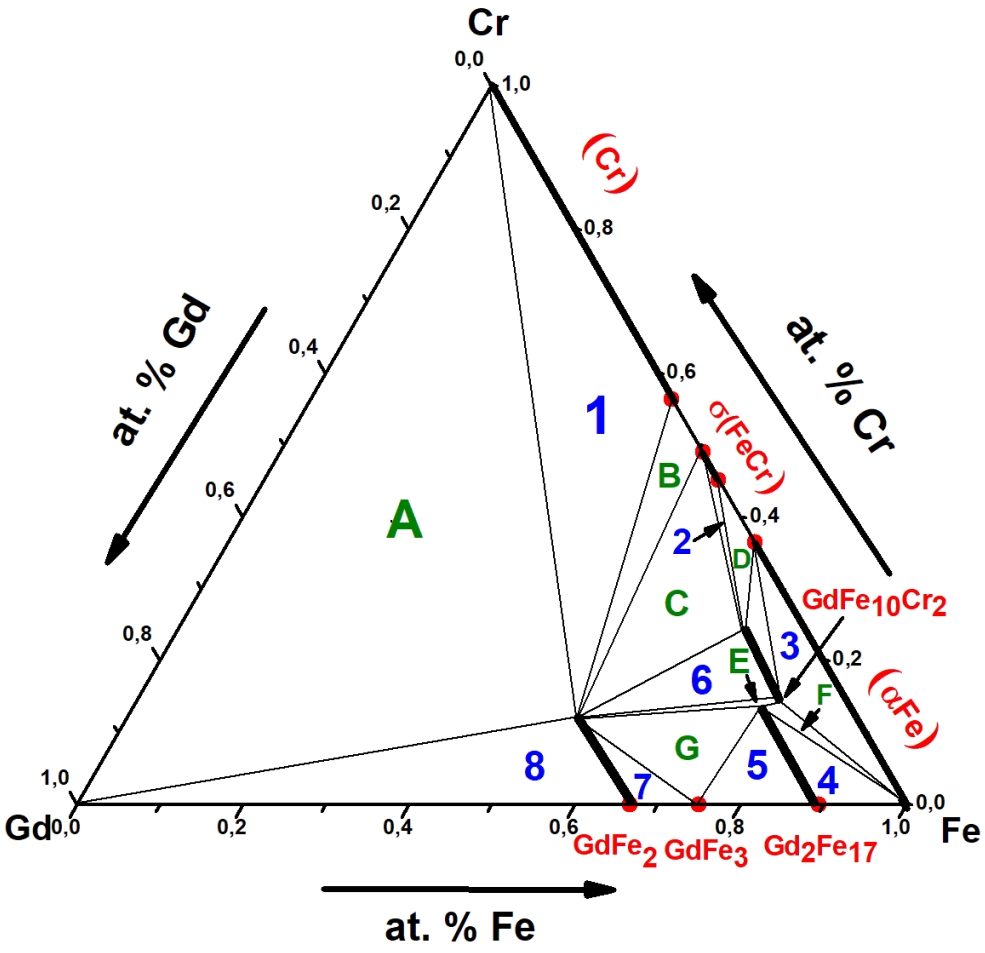

FIG. 20: Isothermal section at 800°C of the Gd-Fe-Cr phase diagram. The areas of the three-phase regions are identified with letters and the areas of the two-phase regions are identified with numbers.

information relating to the solubility limit and phase relations in this ternary system.

IV. CONCLUSIONS

The isothermal section of the phase diagram of Gd-Fe-Cr system was determined at 800°C. It consists of eight single-phase regions, eight two-phase regions and seven three-phase regions. Four binary compounds, namely $GdFe_2$, $GdFe_3$, Gd_2Fe_{17} and σ(FeCr) and one ternary compound, $GdFe_{10}Cr_2$, were confirmed to exist in this section. Conversely, the

binary compound Gd_6Fe_{23} was not found at 800°C. The isothermal section of Gd-Fe-Cr had two binary compounds which extended into the system $GdFe_{2-x}Cr_x$ and $Gd_2Fe_{17-x}Cr_x$. The maximum solid solubilities of Cr in $GdFe_2$ and Gd_2Fe_{17} were about 11.7 at. % Cr and 13.2 at. % Cr respectively. The extent of the ternary coumpound $GdFe_{10}Cr_2$ was observed and its limit of solubility was evaluated: $GdFe_{12-x}Cr_x$ with substitution up to 23.1 at. % Cr.

V. ACKNOWLEDGMENTS

This work was mainly supported by the CNRS, the Tunisian Ministry of Higher Education and Scientific Research and Technology (LAB MESLAB) (Tunisia-Sfax) and the Higher Education, Scientific of French (PHC MAGHREB project 15MAG07).

VI. REFERENCES

[1] S. Yu. Dan´kov, A. M. Tishin, V. K. Pecharsky, and K. A. Gschneidner Jr, Phys. Rev. B. **57** (1998) 3478-3490.

[2] R. Nirmala, A. V. Morozkin, and S. K. Malik, Pramana-J. Phys. **84** (2015) 977-985.

[3] R. Guetari, R. Bez, A. Belhadj, K. Zehani, A. Bezergheanu, N. Mliki, L. Bessais, and C. Cizmas, J. Alloys Compd. **588** (2014) 64-69.

[4] V. K. Pecharsky, and K. A. Gschneidner Jr, J. Magn. Magn. Mater. **200** (1999) 44-56.

[5] R. Vert, D. Fruchart, B. Garcia-Landa, D. Gignoux, and Y. Amako, J. Alloys Compd. **275** (1998) 611-614.

[6] P. Qian, N. X. Chen, and J. Shen, Solid State Commun. **134** (2005) 771-776.

[7] D. B. De Mooij, and K. H. J. Buschow, J. Less-Common Met. **136** (1988) 207-215.

[8] R. Verhoef, F. R. De Boer, Z. Zhi-dong, and K. H. J. Buschow, J. Magn. Magn. Mater. **75** (1988) 319-322.

[9] X. P. Zhong, F. R. De Boer, D. B. De Mooij, and K. H. J. Buschow, J. Less-Common Met. **163** (1990) 123-132.

[10] Y. Fu-ming, L. Qing-an, Z. Ru-wen, K. Jian-ping, F. R. De Boer, J. P. Liu, K. V. Rao, G. Nicolaides, and K. H. J. Buschow, J. Alloys Compd. **177** (1991) 93-100.

[11] J. J. Bara, B. F. Bogacz, A. T. Pedziwiatr, P. Stefanski, A. Szlaferek, andA. Wrzeciono, J. Alloys Compd. **265** (1998) 70-79.

[12] L. Bessais, and C. Djega-Mariadassou, Phys. Rev. B. **63** (2001) 054412

[13] S. Khazzan, L. Bessais, G. Van Tendeloo, andN. Mliki, J. Magn. Magn. Mater. **363** (2014) 125-132.

[14] M. Jemmali, S. Walha, M. Pasturel, O. Tougait, R. Hassen, and H. Noël, J. Alloys Compd. **489** (2010) 421-423.

[15] N. Bouchaala, M. Jemmali, K. Nouri, S.Walha, A. B. Salah, and L. Bessais, J. Phase Equilib. Diffus **38** (2017) 561-567.

[16] K. Nouri, M. Jemmali, S. Walha,, K. Zehani, A. B. Salah, and L. Bessais, J. Alloys Compd. **661** (2016) 508-515.

[17] M. Jemmali, S. Walha, R. Hassen, and H. Noël, Asian J. Chem. **28** (2016) 1330-1334.

[18] K. Nouri, M. Jemmali, S. Walha, A. B. Salah, E. Dhahri, and L. Bessais, J. Alloys Compd. **719** (2017) 256-263.

[19] Y. Zhong, H. Y. Zhou, C. H Hu, and S. K. Pan, J. Alloys Compd. **541** (2012) 198-203.

[20] Q. R. Yao, H. L Wang, Z. W liu, H. Y. Zhou, and S. K. Pan, J. Alloys Compd. **475** (2009) 286-288.

[21] Q. R. Yao, H. Y. Zhou, S. K. Pan, and Z. M. Wang, J. Alloys Compd. **509** (2011) 1579-1581.

[22] S. K. Pan, X. Liu, L. Cheng, X. K. Wang, Q. R. Yao, and H. Y. Zhou, J. Alloys Compd. **605** (2014) 164-167.

[23] W. He, X. Wang, J. He, J. Wen, M. Yu, and L. Zeng, J. Alloys Compd. **502** (2010) 87-91.

[24] V. F. Novy, R. C. Vickery, and E. V. Kleber, Trans. Metall. Soc. AIME. **221** (1961) 588-590.

[25] M. Copeland and H. Kato, Proceedings of the Conference on Rare Earth Research, 2nd Colorado.Gordon and Breach Science Publishers. pp. (1962) 133-141.

[26] E. M. Savitskii, V. F. Terekhova, R. S. Torchinova, I. A. Markova, O. P. Naumkin, V. Kolesnichenko, and V. F. Stroganova, Handbook on the Physics and Chemistry of Rare-Earths. **180** (1970) 47-60.

[27] W. Zhang, and K. Han, J. Phase Equilib. **19** (1998) 56-63.

[28] R. P. Elliott, Constitution of Binary Alloys, McGraw-Hill, New York. (1965).

[29] T. B. Massalski, H. Okamoto, P. R. Subramanian and L. Kacprzak, Binary Alloy Phase Diagrams, ASM International, Materials Park (1990).

[30] W. Kraus and J. Nolze, Powder Diffr. **13** (1998) 256-259.

[31] J. Rodriguez-Carvajal, FULLPROF: A program for Rietveld Refinement and Pattern Matching analysis-in Abstracts of the Satellite Meeting on Powder Diffraction of the XVth IUCr Congress, Toulouse, France. (1990) 127-128.

[32] M. Saidi, S. Walha, N. Nouri, A. Kabadou, M. Jemmali, and L. Bessais, J. Alloys Compd. **781** (2019) 159-165.

[33] Ye. V. Shcherbakova, G. V. Ivanova, N. V. Mushnikov, I. V. Gervasieva, and A. Bezergheanu, J. Alloys Compd. **308** (2000) 15-20.

[34] A. M Gabay, and G. C. Hadjipanayis, Scr. Mater. **154** (2018) 284-288.

[35] J. V. Florio, R. E. Rundle, and A. I. Snow, Acta cryst. **5** (1952) 449-457.

[36] N. Mattern, M. Zinkevich, A. Handstein, W. Gruner, S. Roth, and O. Gutfleisch, J. Alloys Compd. **358** (2003) 1-6.

[37] J. F. Smith and D. A. Hansen, Acta Crystallogr. **19** (1965) 1019-1024.

[38] K. Mori, H. Onodera, K. Aoki, and T. Masumoto, J. Alloys Compd. **270** (1998) 35-41.

[39] G. Hausch, and E. Toëroëk, Phys. Status Solidi A. **40** (1977) 55-62.

[40] B. J. Beaudry, and A. H. Daane, J. Less-Common. Met. **6** (1964) 322-325.

[41] P. Karen, J. Solid State Chem. **177** (2004) 281-292.

[42] M. Bououdina, H. Enoki, and E. Akiba, J. Alloys Compd. **281** (1998) 290-300.